PARAMETER ESTIMATION TECHNIQUE FOR DOUBLE-DIODE MODEL OF PHOTOVOLTAIC MODULES

Aguinaldo J. Nascimento Junior[1], Marcelo C. Cavalcanti[1], Fabricio Bradaschia[1]
Emerson A. Silva[1], Leandro Michels[2], Luiz P. Pietta Junior[2]
GEPAE - Grupo de Eletrônica de Potência e Acionamentos Elétricos
DEE, UFPE, Recife PE, Brazil
e-mail: aguinaldojunior10@hotmail.com, marcelo.ccavalcanti@ufpe.br, fabricio.bradaschia@ufpe.br

***Abstract* - This paper proposes a parameter estimation technique for the double-diode electrical model based on the physical behavior of the photovoltaic (PV) module with respect to variations of the environmental conditions. There are several different techniques for PV parameter estimation. However, most of them identify the parameters for a specific irradiance and temperature. This means that different sets of parameters are found for each environmental condition, providing results that do not represent I-V curves correctly. Thus, the parameters provide only a mathematical representation with lack of physical meaning. In the proposed technique, it is necessary to execute the parameter estimation only once, because the model is valid for all range of values of the environmental conditions available on datasheets or experimental curves. Moreover, the restrictions imposed on each parameter makes the model capable of emulating the physical behavior of the PV module, particularly useful in fault diagnosis and predictive and corrective maintenance of PV systems. Comparison results based on datasheet and experimental curves are presented to verify the effectiveness of the proposed parameter estimation technique.**

***Keywords* – Parameter estimation, PV cells, PV systems.**

I. INTRODUCTION

Mathematical models for PV cells/modules are very relevant when necessary a better understanding of its working. These models have been used to accurately predict the electrical power produced from PV arrays, for simulations of PV arrays under different weather conditions, and for design and optimization of maximum power point (MPP) tracking (MPPT) techniques [1].

PV modules present current-voltage (I-V) relationships with nonlinear properties that depend on their constructive characteristics as well as the environmental conditions. Most models for PV cells are based on electrical equivalent circuits that use a set of parameters to represent their I-V relationships. Based on the physical interpretation of a PV cell and its arrangement to form a module, two equivalent electrical models can be built: the single-diode and double-diode models. Figure 1 shows the double-diode equivalent electrical circuit of the PV cell, which is comprised of a photogenerated current source (I_g), two anti-parallel diodes (d_1), (d_2), a series resistance (R_s) and a shunt resistance (R_p).

The determination of parameters for the models of PV cells by analytical techniques [2, 3] is complex since their I-V relationships are described by a set of nonlinear equations which parameters are reciprocally coupled. Due to this complexity, several different techniques to determine these parameters have been proposed in literature. Some techniques are based on numerical solutions or iterative algorithms to determine the values of the seven [4], five [5] or four [6, 7] parameters, where a system of equations is derived for specific operating points provided in datasheets of commercial modules, such as the short-circuit (SC), open-circuit (OC) and maximum power (MP) operating points.

However, under some specific conditions, the traditional techniques may provide PV parameters with no physical meaning. For example, in [5] the authors consider that the value found for R_s in the standard test conditions (STC) is the same for any environmental condition. This simplification contradicts the physical and constructive characteristics of the solar cell [8]. In [6], it is considered that the saturation current of both diodes are equal, different from that determined in [9], where the saturation current is higher in diode d_2 as characteristics of silicon solar cells. Other approaches to determine the model parameters apply a curve fitting [10] or optimization algorithms [11]. These techniques require an I-V curve for each PV module, that may be experimental or provided by manufacturers datasheets.

The major drawback of these techniques is that the determination of the model parameters is only performed at STC. Consequently, it is required to use an extrapolating method based on PV modules datasheet to determine the parameters for different environmental conditions. As a result, different sets of parameters are obtained for each experimental I-V curve. Since the estimated parameters are based only on a mathematical fit, there is no physical interpretation for the

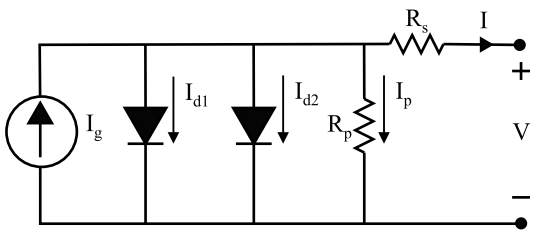

Fig. 1. Equivalent electrical representation of a PV cell.

978-1-5090-6248-5/17/$31.00 © 2017 IEEE

variation in the parameters.

In [10] it was proposed an estimation technique to identify the electrical model parameters presenting some correspondence with the physical behavior of PV modules. The technique was able to find five unknown parameters of the single-diode model from data provided by manufacturers datasheet or experimental curves. The technique was based on a full scan of the possible physical values of the parameters at the STC and considered the dependence of R_s on temperature and irradiance. Although interesting, this technique is limited, since it has not considered the other parameters' dependence on temperature and irradiance, i.e., it could not fully represent the physical phenomena of PV modules.

Besides this limitation, in a real cell, the phenomenon of recombination of charge carriers represents a substantial loss that can not be adequately represented using a single-diode model [5, 12, 13] because it is based on the assumption that the loss by recombination in the depletion region is absent. Thus, to describe more precisely the junction p-n, a second diode is added in the structure. The consideration of this loss leads to a more precise model, known as the double-diode model (Fig. 1). In this model, the diffusion current due to the majority carriers is represented by I_{d1} and flows through the first diode, while the current I_{d2} that flows through the second diode represents the recombination current, due to the minority carriers [5, 12, 13]. The main contribution of this paper is the proposal of a total scan technique for the double-diode equivalent electrical model for PV modules where all parameters depend on temperature (T) and irradiance (S) values.

II. MATHEMATICAL MODELING OF PV MODULES

For the equivalent electric circuit of PV module model (Fig. 1), the current is given as follows:

$$\begin{aligned} I = I_g - I_{01}\left[\exp\left(\frac{V+IR_s}{A_1V_t}\right)-1\right] \\ - I_{02}\left[\exp\left(\frac{V+IR_s}{A_2V_t}\right)-1\right] - \left(\frac{V+IR_s}{R_p}\right) \end{aligned} \quad (1)$$

where V and I are the output voltage and current; N_s is the number of series connected cells; T is the temperature (K); I_{01} and I_{02} are the reverse saturation currents of diffusion and recombination phenomena; A_1 is the ideality factor of diffusion and A_2 is the ideality factor of recombination; V_t is the thermal voltage given by $V_t = N_s kT/q$, k is the Boltzmann constant ($k = 1.38 \times 10^{-23}$ J/K) and q is the electron charge ($q = 1.6 \times 10^{-19}$ C).

Based on the theory of p-n junctions [14] and in the characteristics of silicon cells [9], it is possible to relate the saturation current to the temperature as [5, 12, 13]:

$$\frac{I_{01}}{I_{01,ref}} = \left(\frac{T}{T_{ref}}\right)^{3/A1} \exp\left[\frac{q}{A_1k}\left(\frac{E_{g,ref}}{T_{ref}} - \frac{E_g}{T}\right)\right] \quad (2)$$

where the subscript *ref* is the value of the parameter at the reference environmental condition. E_g is the material band gap energy, also defined as a function of the temperature [15]

$$E_g = E_{g,0} - \frac{aT^2}{T+b} \quad (3)$$

where $E_{g,0}$ is its value at 0 K, and a and b are constants that depend of the material. For silicon $E_{g,0} = 1.1557\,eV$, $a = 7.021 \times 10^{-4}\,eV\mathrm{K}^{-1}$ and $b = 1.108\,\mathrm{K}$.

Usually, it is assumed that only I_g depends on the temperature and irradiation, by using [16]:

$$I_g = [I_{g,ref} + \alpha(T - T_{ref})]\frac{S}{S_{ref}}, \quad (4)$$

where S is the solar irradiance ($\mathrm{W/m^2}$) and α is the temperature coefficient of the SC current ($A/°C$). The resistances and the ideality factors are determined for a reference environmental condition [17]. For other conditions, generally the values found at the reference are repeated or a new estimation process is performed. However, to characterize a PV module, it is important to study the dependence on irradiation and temperature of all parameters of the model.

III. DEPENDENCE ON AMBIENT CONDITIONS OF THE SOLAR CELL PARAMETERS

A. *Dependence on Irradiance of Solar Cell Parameters*

The resistances of the solar cells are parameters that limit their conversion efficiencies. The resistance R_s occurs mainly due to the movement of electrons and the contact metal-silicon of the cell [18]. On the other hand, R_p represents parallel high-conductivity paths across the solar cell. These parallel paths are detrimental to the module performance especially at low irradiances [19]. For an ideal cell, R_s is zero avoiding a voltage drop before the load, and R_p is infinite canceling an alternative path for the current [18]. In real conditions, the increase of R_s and the decrease of R_p cause a reduction in the power and efficiency of the solar cell.

Consequently, it is necessary a special attention when modeling these parameters, verifying if there are interferences of external factors in their values. Some authors attribute the increase of the conductivity of the active layer with the increase of S, as one of the reasons for the decrease of R_s. The rate of decrease is faster at low values of S, becoming smaller for higher S values [20], [21]. This implies $\gamma_{Rs} < 0$ in:

$$R_s(S) = R_{s,ref1}\left(\frac{S}{S_{ref}}\right)^{\gamma_{Rs}} + R_{s,ref2}. \quad (5)$$

In this paper, this behavior is confirmed through a process of parameter estimation performed in some modules for each one of the curves that represent the module for irradiance variations, provided in their datasheets. Therefore, it results in a power trend line for T constant, that is in accordance with some results found in the literature [18, 22, 23].

On the other hand, R_p increases at low S values. Conceptually, R_p is related to the constructive characteristics of the p-n junction. Thereby, a concentration of traps, present in the regions of localized defects, act as collector for photo-generated minority charge carriers. As S increases the traps begin to be filled, so that after filling all traps, R_p reaches its maximum

value. Thereafter, further increases of S at higher levels induce degradation in the PV solar cell, causing the decrease of R_p [18, 21, 24] and consequently implying in $\gamma_{Rp} < 0$ in:

$$R_p(S) = R_{p,ref}\left(\frac{S}{S_{ref}}\right)^{\gamma_{Rp}}. \tag{6}$$

In this paper, this behavior is confirmed through the same process of parameter estimation performed in some modules. As result of this, it is also possible to express this behavior as a power trend line for T constant, that is also in accordance with some results found in the literature [23, 25].

B. Dependence on Temperature of Solar Cell Parameters

When the temperature increases, the MP of the cells decreases, especially due to the reduction of the OC voltage [18]. Some studies presented in [26] show that R_s is a thermal sensitive resistance that belongs to the form of the positive temperature coefficient type. They indicate an exponential or approximately linear growth of R_s with increasing temperature [23, 26, 27]. The authors in [20] claim that there is a minimum value for R_s at a particular temperature, and that increasing or decreasing temperature from that point causes R_s to increase. This behavior is explained in terms of the various contributions to the series resistance, such that above ambient temperature the sheet resistance of the diffusion layer becomes dominant and R_s increases with temperature, implying $k_{Rs} > 0$ in:

$$R_s(T) = R_{s,ref1} + R_{s,ref2}[1 + k_{Rs}(T - T_{ref})]. \tag{7}$$

In this paper, this behavior is confirmed through the process of parameter estimation in the previous subsection, that was repeated, but this time for curves of different temperatures. Though the physical structure of R_s of the cell is complicated, with influence of base contact, base bulk, sheet and metallic resistances, (7) is a theoretical equation based on these factors and may accurately predict the values of R_s [26]. A similar conclusion can be found in [18, 23, 27].

On the other hand, the effect of temperature on R_p is similar to the effect caused by high S. Previous researches report that R_p decreases monotonically with temperature [23, 28]. The rate of decrease is faster at low T values exhibiting an approximately linear behavior, especially at temperatures higher than ambient temperature [27,28]. This is interpreted as a combination of tunnelling and trapping-detrapping of carriers through the defect states that act as recombination centres or traps [29]. From this analysis it can be inferred that $k_{Rp} < 0$ in:

$$R_p(T) = R_{p,ref}[1 + k_{Rp}(T - T_{ref})]. \tag{8}$$

In this paper, this behavior is confirmed through a process of parameter estimation performed in some modules. As result of this, it is possible to express this behavior as a linear trend line for S constant. This is also in accordance with some results found in the literature [18, 27, 29].

IV. PROPOSED TECHNIQUE

The proposed technique in this paper tries to solve the limitations found in the techniques that do not consider the influence of environmental conditions on the electrical parameters of the PV model. For this, a total scan of all possible values of R_s (from 0 to 2 with a step of $1\,m\Omega$), I_g (from I_{sc} to $I_{sc} + 0.5\,A$ with a step of $1\,mA$) and A_1, A_2 (from 1 to 2 with a step of 0.1) is performed, making it possible to calculate R_p through an approximate equation, since it is not possible to write a complete equation as a function only of known parameters and a scan in values of R_p makes the computational cost unfeasible, since it presents larger magnitudes than those of the R_s values. Besides R_p, the saturation currents are also calculated by equations.

Using the characteristic conditions of current and voltage $(0, I_{sc})$, $(V_{oc}, 0)$, (V_{mp}, I_{mp}), available on datasheets, (1) yields to the following equations:

$$\begin{aligned} I_{sc} = I_g - I_{01}&\left[\exp\left(\frac{I_{sc}R_s}{A_1V_t}\right) - 1\right] \\ &- I_{02}\left[\exp\left(\frac{I_{sc}R_s}{A_2V_t}\right) - 1\right] - \frac{I_{sc}R_s}{R_p} \end{aligned} \tag{9}$$

$$\begin{aligned} 0 = I_g - I_{01}&\left[\exp\left(\frac{V_{oc}}{A_1V_t}\right) - 1\right] \\ &- I_{02}\left[\exp\left(\frac{V_{oc}}{A_2V_t}\right) - 1\right] - \frac{V_{oc}}{R_p} \end{aligned} \tag{10}$$

$$\begin{aligned} I_{mp} = I_g - I_{01}&\left[\exp\left(\frac{V_{mp} + I_{mp}R_s}{A_1V_t}\right) - 1\right] \\ &- I_{02}\left[\exp\left(\frac{V_{mp} + I_{mp}R_s}{A_2V_t}\right) - 1\right] - \left(\frac{V_{mp} + I_{mp}R_s}{R_p}\right). \end{aligned} \tag{11}$$

Using the approximation:

$$I_{01}\left[\exp\left(\frac{I_{sc}R_s}{A_1V_t}\right) - 1\right] + I_{02}\left[\exp\left(\frac{I_{sc}R_s}{A_2V_t}\right) - 1\right] \ll 1 \tag{12}$$

in (9), it implies that:

$$R_p \approx \frac{R_sI_{sc}}{I_g - I_{sc}}. \tag{13}$$

To determine I_{01} a combination of (10) and (11) is performed. This implies:

$$I_{01} = \frac{N}{D} \tag{14}$$

where

$$\begin{aligned} N = \left(\frac{V_{oc}}{R_p} - I_g\right)&\left[\frac{\exp\left(\frac{V_{mp}+I_{mp}R_s}{A_2V_t}\right) - 1}{\exp\left(\frac{V_{oc}}{A_2V_t}\right) - 1}\right] \\ &+ I_g - \frac{V_{mp}}{R_p} - I_{mp}\left(1 + \frac{R_s}{R_p}\right) \end{aligned} \tag{15}$$

$$\begin{aligned} D = \left[1 - \exp\left(\frac{V_{oc}}{A_1V_t}\right)\right]&\left[\frac{\exp\left(\frac{V_{mp}+I_{mp}R_s}{A_2V_t}\right) - 1}{\exp\left(\frac{V_{oc}}{A_2V_t}\right) - 1}\right] \\ &+ \left[\exp\left(\frac{V_{mp} + I_{mp}R_s)}{A_1V_t}\right) - 1\right]. \end{aligned} \tag{16}$$

Using (10), one can determine I_{02} as

$$I_{02} = \frac{I_g - \frac{V_{oc}}{R_p} - I_{01}\left[\exp\left(\frac{V_{oc}}{A_1 V_t}\right) - 1\right]}{\exp\left(\frac{V_{oc}}{A_2 V_t}\right) - 1}. \quad (17)$$

With all parameters determined, the relation given in (1) can be solved and the best set of parameters can be chosen based on the lowest value of the mean absolute error in power (MAEP) calculated between the curve generated by the electric model and from the datasheet curve or from the experimental curve. The flowchart of the proposed technique is seen in Figure 2.

This metric that uses the P-V curves instead of I-V curves on conventional metrics, has already been discussed in [10]. The motivation for this metric is that most applications for the PV electrical model need accurate values of the generated power. The absolute error in power for a specific voltage point is calculated by:

$$error = |P_{curve} - P_{model}| \quad (18)$$

where P_{curve} is the product of V_{curve} and I_{curve} obtained by the datasheet or experimental curve; and P_{model} is the product of V_{model} and I_{model} obtained by the simulation of the electrical model with the parameters estimated by the proposed technique.

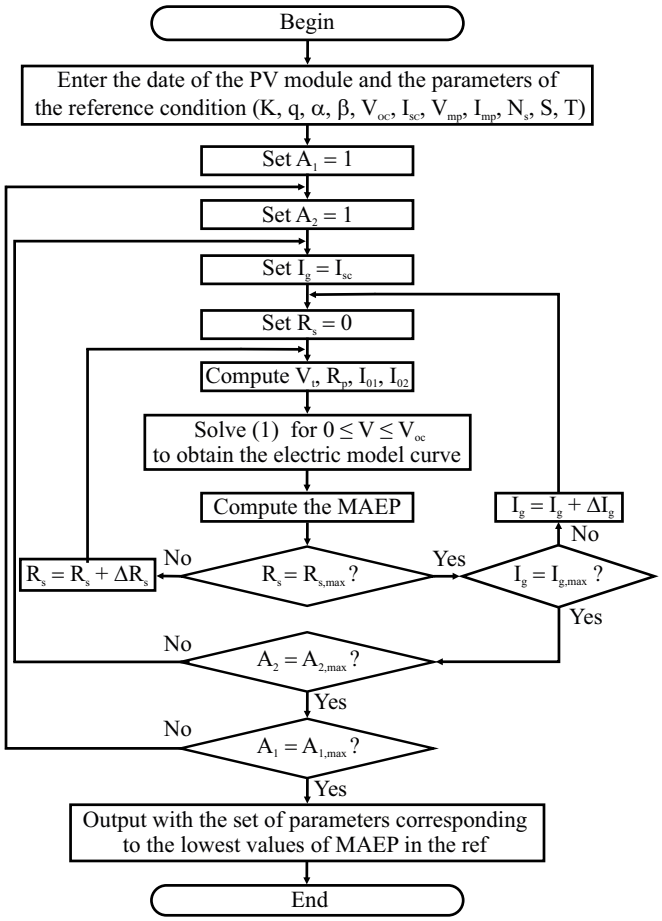

Fig. 2. Proposed technique flowchart.

The MAEP is calculated by:

$$MAEP = \frac{\sum_{n=1}^{N_p} error_n}{N_p} \quad (19)$$

where $error$ is calculated for all voltage points going from zero to the OC condition and N_p is the number of voltage points extracted from the datasheet or experimental I-V curve of the PV module.

After obtaining all parameters for reference environmental condition one can determined the k_{Rs}, k_{Rp}, γ_{Rs} and γ_{Rp} coefficients in (7) and (8). For this, it is considered that $A_1 = A_{1,ref}$ and $A_2 = A_{2,ref}$. Furthermore, (2), (4) and (17) are calculated for different conditions of reference. Thus, an equation for V_{oc} is required and a curve-fitting algorithm is carried with all S-dependent V_{oc} values, along with linear variation with temperature resulting in:

$$V_{OC} = V_{OC,ref} + \beta(T - T_{ref}) + k_{Voc} T \ln\left(\frac{S}{S_{ref}}\right) \quad (20)$$

where β is the temperature coefficient of the OC voltage and k_{Voc} is the parameter of OC voltage correction with S.

For obtaining the k_{Rs} and k_{Rp} coefficients, the P-V curves are built for each k_{Rs} and k_{Rp} changing from 0 to $10\,\%/°C$ with a step of $0.1\,\%/°C$. Thus, using all available temperature conditions in the datasheet with constant irradiance, the coefficients k_{Rs} and k_{Rp} related to the lowest mean value of MAEP are chosen.

The coefficients γ_{Rs} and γ_{Rp} are determined after R_s and R_p being obtained through complete scans at different irradiance and the same temperature. This process is similar to that described in Figure 2. Thus, a curve-fitting algorithm is carried with all the best values of R_s and R_p, determining an adjusted value for the coefficients.

V. COMPARISON RESULTS

Some techniques in literature are implemented for comparison by using MATLAB. Two results are shown in this section. The first case is for the datasheet curves, obtained by a curve extractor algorithm developed in MATLAB through image processing, and the second one is for experimental curves, obtained through a curve extractor prototype, that include irradiance and temperature sensors together with accurate voltage and current probes to measure the output voltage and current during charging/discharging capacitors.

A. PV Module KC200GT - Datasheet Curves

Table I shows the comparison results obtained for the module KC200GT, a multicrystal PV module from Kyocera. The results of all parameters were estimated at the reference condition, defined as $S_{ref} = 1000\,W/m^2$ and $T_{ref} = 25\,°C$.

The remaining parameters found for the proposed method: $R_{s,ref1} = 0.13\,m\Omega$; $R_{s,ref2} = 0.126\,m\Omega$; $k_{Rs} = 0.3\,\%/°C$; $k_{Rp} = 0.4\,\%/°C$; $\gamma_{Rs} = 1.28$; $\gamma_{Rp} = 1.57$. As can be seen in Table I, the proposed model did not obtain the best result in the reference condition, presenting the second lowest value of $MAEP$ among the simulated techniques.

However, as can be seen in Table I and in the Figures 3 and 4,the proposed model present the best performance for seven

TABLE I: Estimation techniques comparison for module KC200GT

Parameter	Techiniques*			
	A	**B**	**C**	**D**
A_1	1	1	1	1
A_2	-	2	2	1.7
$R_s\ (m\Omega)$	0.256	0.268	0.262	0.256
$R_p\ (\Omega)$	149.94	201.52	312.72	139.68
$I_g\ (A)$	8.19	8.19	8.19	8.2
$I_{01}\ (A)$	3.4×10^{-10}	3.5×10^{-10}	3.2×10^{-10}	3.4×10^{-10}
$I_{02}\ (A)$	-	3.5×10^{-10}	3.43×10^{-6}	6.32×10^{-9}
$MAEP_{ref}(W)$	**0.40**	0.92	0.93	0.44
$MAEP_{av}(W)$	0.67	1.03	1.79	**0.49**

Techiques*: A - Total Scan [10], B - Ishaque [6], C - Hejri [5], D - Proposal.

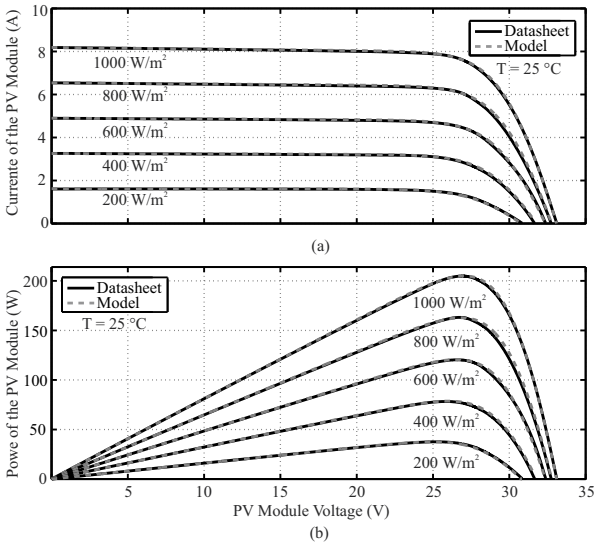

Fig. 3. Comparison between the proposed technique and datasheet curves for module KC200GT at different irradiances, $25\,°C$.

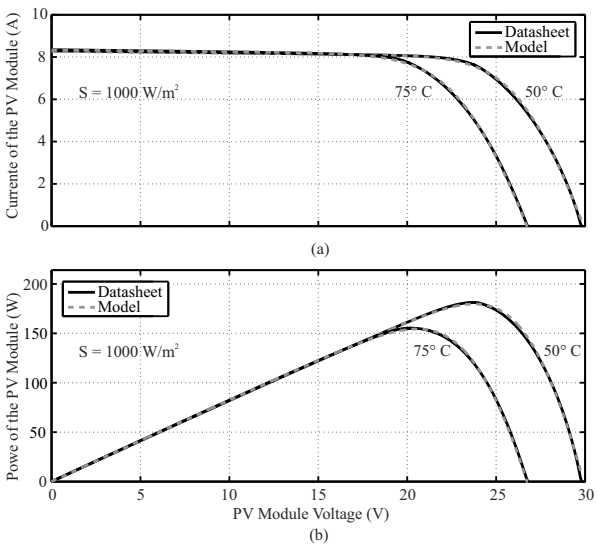

Fig. 4. Comparison between the proposed technique and datasheet curves for module KC200GT at different temperatures, $1000\,W/m^2$.

curves at different temperature and irradiance conditions, presenting o lowest value of $MAEP_{av}$.

TABLE II: Estimation techniques comparison for module GBR255

Parameter	Techiniques*			
	A	**B**	**C**	**D**
A_1	1.8	1	1	1
A_2	-	2	2	1.8
$R_s\ (m\Omega)$	0.43	0.75	0.76	0.43
$R_p\ (\Omega)$	1.23×10^4	138	170.2	∞
$I_g\ (A)$	8.82	8.82	8.86	8.82
$I_{01}\ (A)$	6.86×10^{-5}	5.62×10^{-9}	5.2×10^{-9}	2.08×10^{-12}
$I_{02}\ (A)$	-	5.62×10^{-9}	1.22×10^{-5}	6.86×10^{-5}
$MAEP_{ref}(W)$	**1.57**	7	6	**1.57**
$MAEP_{av}(W)$	2.26	8	11	**2.11**

Techiques*: A - Total Scan [10], B - Ishaque [6], C - Hejri [5], D - Proposal.

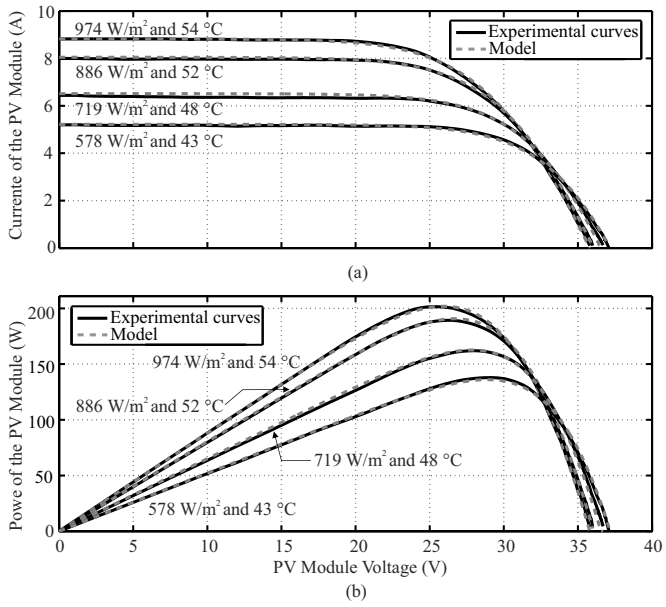

Fig. 5. Comparison between the proposed technique and the experimental curves for the module GBR255 at different irradiances and temperatures.

B. PV Module GBR255 - Experimental Curves

Table II shows the comparison results obtained for the module GBR255, a poly crystalline PV module from Globo Brasil. All parameters were estimated at the reference condition, defined as $S_{ref} = 970\,W/m^2$ and $T = 54\,°C$.

The remaining parameters found for the proposed method: $R_{s,ref1} = 0.157\,m\Omega$; $R_{s,ref2} = 0.273\,m\Omega$; $k_{Rs} = 15\,\%/°C$; $\gamma_{Rs} = 2.17$. As can be seen in Table II and Figure 5, the proposed model obtained the best result of $MAEP$ at the reference condition and the lowest $MAEP_{av}$ for the four curves at different temperature and irradiance conditions from each PV module.

VI. CONCLUSION

This paper proposes an accurate parameter estimation technique for the double-diode model. This new approach presented superior results when compared with well-known techniques, showing that the proposed total scan is effective in em-

ulating the physical behavior of modules, particularly useful in fault diagnosis and predictive and corrective maintenance of photovoltaic systems.

REFERENCES

[1] K. Rhle, M. K. Juhl, M. D. Abbott, and M. Kasemann. Evaluating Crystalline Silicon Solar Cells at Low Light Intensities Using Intensity-Dependent Analysis of I-V Parameters. *IEEE J. Photovolt.*, 5(3):926–931, May 2015.

[2] S. Shongwe and M. Hanif. Comparative Analysis of Different Single-Diode PV Modeling Methods. *IEEE J. Photovolt.*, 5(3):938–946, May 2015.

[3] D. S. H. Chan and J. C. H. Phang. Analytical methods for the extraction of solar-cell single- and double-diode model parameters from i-v characteristics. *IEEE Transactions on Electron Devices*, 34(2):286–293, Feb 1987.

[4] Adel A. Elbaset, Hamdi Ali, and Montaser Abd-El Sattar. Novel seven-parameter model for photovoltaic modules. *Solar Energy Materials and Solar Cells*, 130:442 – 455, 2014.

[5] M. Hejri, H. Mokhtari, M. R. Azizian, M. Ghandhari, and L. Soder. On the parameter extraction of a five-parameter double-diode model of photovoltaic cells and modules. *IEEE Journal of Photovoltaics*, 4(3):915–923, May 2014.

[6] Kashif Ishaque, Zainal Salam, and Hamed Taheri. Simple, fast and accurate two-diode model for photovoltaic modules. *Solar Energy Materials and Solar Cells*, 95(2):586 – 594, February 2011.

[7] M. G. Villalva, J. R. Gazoli, and E. R. Filho. Comprehensive approach to modeling and simulation of photovoltaic arrays. *IEEE Transactions on Power Electronics*, 24(5):1198–1208, May 2009.

[8] J. D. Arora, A. V. Verma, and Mala Bhatnagar. Variation of series resistance with temperature and illumination level in diffused junction poly- and single-crystalline silicon solar cells. *Journal of Materials Science Letters*, 5(12):1210–1212.

[9] M. Wolf, G. T. Noel, and R. J. Stirn. Investigation of the double exponential in the current-voltage characteristics of silicon solar cells. *IEEE Transactions on Electron Devices*, 24(4):419–428, Apr 1977.

[10] E. A. Silva, F. Bradaschia, M. C. Cavalcanti, and A. J. Nascimento. Parameter Estimation Method to Improve the Accuracy of Photovoltaic Electrical Model. *IEEE J. Photovolt.*, 6(1):278–285, Jan 2016.

[11] J. J. Soon and K. S. Low. Photovoltaic Model Identification Using Particle Swarm Optimization With Inverse Barrier Constraint. *IEEE Trans. Power Electron.*, 27(9):3975–3983, Sept 2012.

[12] R.A. Messenger and J. Ventre. *Photovoltaic Systems Engineering, Second Edition*. Taylor & Francis, 2003.

[13] W. De Soto, S.A. Klein, and W.A. Beckman. Improvement and validation of a model for photovoltaic array performance. *Solar Energy*, 80(1):78 – 88, 2006.

[14] W. Shockley. The theory of p-n junctions in semiconductors and p-n junction transistors. *The Bell System Technical Journal*, 28(3):435–489, July 1949.

[15] Y.P. Varshni. Temperature dependence of the energy gap in semiconductors. *Physica*, 34(1):149 – 154, 1967.

[16] Ali Naci Celik and Nasr Acikgoz. Modelling and experimental verification of the operating current of monocrystalline photovoltaic modules using four- and five-parameter models. *Applied Energy*, 84(1):1 – 15, 2007.

[17] Engin Karatepe, Mutlu Boztepe, and Metin Colak. Neural network based solar cell model. *Energy Conversion and Management*, 47(910):1159 – 1178, 2006.

[18] W. Abd El-Basit, A. M. Abd ElMaksood, and F. A. E.-M. S. Soliman. Mathematical Model for Photovoltaic Cells. *Leonardo Journal of Sciences*, 23:13–28, 2013.

[19] L. Pan. Analysis of Photovoltaic Module Resistance Characteristics. *International Journal of Engineering*, 26(11):1369–1376, 2013.

[20] J. D. Arora, A. V. Verma, and M. Bhatnagar. Variation of series resistance with temperature and illumination level in diffused junction poly- and single-crystalline silicon solar cells. *Journal of Materials Science Letters*, 5(12):1210–1212, 1986.

[21] F. Khan, S.-H. Baek, and J. H. Kim. Intensity dependency of photovoltaic cell parameters under high illumination conditions: An analysis. *Applied Energy*, 133:356–362, 2014.

[22] L. Cerna, V. Benda, and Z. Machacek. A note on irradiance dependence of photovoltaic cell and module parameters. In *28th ICM*, pages 273–276, May 2012.

[23] E. Karatepe, M. Boztepe, and M. Colak. Neural network based solar cell model. *Energy Conversion and Management*, 47(9-10):1159–1178, 2006.

[24] C.-T. Sah, R. N. Noyce, and W. Shockley. Carrier generation and recombination in p-n junctions and p-n junction characteristics. *Proceedings of the IRE*, 45(9):1228–1243, September 1957.

[25] A. Mermoud and T. Lejeune. Performance assessment of a simulation model for PV modules of any available technology. In *25th EU PVSEC*, September 2010.

[26] J. Ding, X. Cheng, and T. Fu. Analysis of series resistance and P-T characteristics of the solar cell. *Vacuum*, 2(77):163–167, 2005.

[27] S. Bensalem and M. Chegaar. Thermal behavior of parasitic resistances of polycrystalline silicon solar cells. *Revue des Energies Renouvelables*, 16(1):171–176, 2013.

[28] K. Nishioka, N. Sakitani, K. I. Kurobe, Y. Yamamoto, Y. Ishikawa, Y. Uraoka, and T. Fuyuki. Analysis of the temperature characteristics in polycrystalline si solar cells using modified equivalent circuit model. *Japanese Journal of Applied Physics*, 42(12):71–75, 2003.

[29] E. Cuce, P. M. Cuce, and T. Bali. An experimental analysis of illumination intensity and temperature dependency of photovoltaic cell parameters. *Applied Energy*, 111:374–382, 2013.